Transverse Distance Between the Membrane and the Agonist Binding Sites on the *Torpedo* Acetylcholine Receptor: A Fluorescence Study

C. Fernando Valenzuela, Phi Weign, Juan Yguerabide, and David A. Johnson
Division of Biomedical Sciences and Department of Neuroscience University of California, Riverside, California 92521-0121; and Department of Biology, University of California, San Diego, La Jolla, California 92093 USA

ABSTRACT Fluorescence dipolar resonance energy transfer between a receptor-bound fluorescent agonist, dansyl-C_6-choline, and two membrane-partitioned fluorescent probes, C_{18}-rhodamine and C_{12}-eosin, was used to measure the transverse distance between the acetylcholine (ACh) binding sites on the intact *Torpedo* nicotinic acetylcholine receptor (nAChR) and the surface of the lipid membrane. Control experiments demonstrated that: (1) dansyl-C_6-choline binds to cobra-α-toxin sensitive sites on the nAChR with a $K_D \approx 20$ nM, (2) the quantum yield of dansyl-C_6-choline increases 3.1-fold upon binding, and (3) the receptor-bound dansyl-C_6-choline fluorescence is stable for at least 2 h. The calculated transverse distances between receptor-bound dansyl-C_6-choline and the membrane-partitioned acceptors, C_{12}-eosin and C_{18}-rhodamine, were 31 and 39 Å, respectively. Therefore, given the dimensions of the extracellular domain of the receptor, the ACh binding sites are located significantly below (~25 Å) the extracellular apex of the nAChR. These results are in agreement with the recent proposed location for the ACh binding sites in a pocket within each of the two α-subunits, ~30 Å above the membrane surface (Unwin, N. (1993) *J. Mol. Biol.* 229: 1101–1124).

INTRODUCTION

The nicotinic acetylcholine receptor (nAChR) is a member of the family of ion-gated channels that includes the $GABA_A$, glycine, and serotonin ($5\text{-}HT_3$) receptors (Stroud et al., 1990). The muscle-type nAChR isolated from the *Torpedo* electroplax is the best characterized member of this family. It is formed by four types of subunits denoted as α, β, γ, and δ in a stoichiometric ratio of 2:1:1:1, respectively. Agonists and competitive antagonists bind to two sites/receptor functional unit (Galzi, et al., 1991). The agonist-competitive antagonist or acetylcholine (ACh) binding sites are primarily formed by the two α-subunits (see Karlin, 1991, for a review); however, the δ, γ, and β subunits appear to contribute to the formation of the ACh binding sites (Chatrenet et al., 1990; Pedersen and Cohen, 1990). In addition to the agonist/competitive antagonist binding sites, there exists a class of high-affinity noncompetitive inhibitor (HNCI) binding sites that are generally thought to be located in the transmembrane domain of the receptor (Taylor et al., 1991). Many organic cations can interact with both classes of binding sites if present in sufficiently high concentrations.

The location of the ACh binding sites relative to the quaternary structure of the nAChR has been investigated by using various approaches. Electron microscopic studies of membrane-associated nAChR (Klymkowsky et al., 1979; Zingsheim et al., 1982) or tubular crystals of nAChR (Kubalek et al., 1987) and x-ray diffraction studies (Kistler et al., 1982; Mitra et al., 1989) suggest that the competitive antagonist, α-bungarotoxin, binds at the extracellular apex of the receptor. Fluorescence resonance energy transfer (FRET) measurements, on the other hand, point to a location of the ACh binding sites significantly below the extracellular apex. The distance between the ACh binding sites and the HNCI binding site for ethidium was found to be only 21–40 Å (Herz et al., 1989). Given that 1) ethidium is a voltage-dependent channel blocker that probably binds to the transmembrane region of the receptor (Sterz et al., 1982; Herz et al., 1987, 1991, 1992), and 2) the receptor protrudes 55–65 Å out of the extracellular side of the membrane (Kistler et al., 1982; Toyoshima and Unwin, 1990), this FRET study suggests that the ACh binding sites are located ~22–45 Å below the extracellular apex of the nAChR.

Similarly, Johnson et al. (1990) measured with FRET the distance from sites of fluorescein labeling on receptor-bound cobra-α-toxin to the membrane surface. The calculated transverse distance between these sites on the cobra-α-toxin and the membrane surface ranged between 39 and 45 Å. Given the size of the α-toxin ($20 \times 30 \times 40$ Å (Walkinshaw et al., 1980)) and its deduced orientation on the nAChR (Johnson et al., 1990), the ACh binding sites would appear to be located ~30 Å above the membrane surface, and therefore well

Received for publication 23 September 1993 and in final form 30 December 1993.

Address reprint requests to Dr. David A. Johnson, Division of Biomedical Sciences, University of California, Riverside, CA 92521-0121. Tel.: 909-787-3831; Fax: 909-787-5504.

This work was supported by the American Heart Association (California Affiliate) Grant 91-140 to D.A.J.

The abbreviations and trivial names used are: ACh, acetylcholine; nAChR, nicotinic acetylcholine receptor; Buffer I, 100 mm NaCl and 10 mM sodium phosphate, pH 7.4; C_{12}-eosin, 5-(*N*-dodecanoyl)aminoeosin; C_{12}-fluorescein, 5-(*N*-dodecanoyl)aminofluorescein; C_{18}-rhodamine, octadecyl rhodamine B; dansyl-C_6-choline, 6-(5-dimethylaminonaphtalene-1-sulfonamido)hexanoic acid-β-(*N*-trimethylamonium) ethyl ester; dansyltrimethylamine, dimethylaminonaphthalene-5-sulphonamidoethyltrimetylammonium; FRET, fluorescence resonance energy transfer; HNCI, high-affinity noncompetitive inhibitor; PCP, phencyclidine.

0006-3495/94/03/674/09 $2.00

below the extracellular apex. However, the lack of confirmation of the proposed orientation of the bound cobra-α-toxin (Johnson et al., 1990) necessitates the use of an approach that is independent of the α-toxin orientation.

Toward this end, we report here the use of a relatively small fluorescent nicotinic agonist, dansyl-C_6-choline, as an electronic energy donor to two membrane-partitioned acceptors, octadecyl rhodamine B (C_{18}-rhodamine) and 5-(*N*-dodecanoyl)aminoeosin (C_{12}-eosin). These acceptors are composed of a charged fluorophore attached to a hydrocarbon membrane anchor. With such a molecular configuration these probes would be expected, upon partitioning into membranes, to position themselves at the water-lipid interface and, thus, allow transverse distance measurements between the agonist sites and the surface of the lipid membrane.

EXPERIMENTAL PROCEDURES

Materials

5-(*N*-Dodecanoyl)aminofluorescein (C_{12}-fluorescein), C_{12}-eosin, and C_{18}-rhodamine were purchased from Molecular Probes (Eugene, OR). *Torpedo californica* electric rays were obtained from Marinus Inc. (Long Beach, CA). Phencyclidine (PCP) and suberyldicholine were from Sigma (St. Louis, MO). Cobra-α-toxin was isolated following the method of Karlsson et al. (1971) from *Naja naja siamensis* venom purchased from the Miami Serpentarium (Salt Lake city, UT). Dansyltrimethylamine perchlorate was acquired from Pierce Chemical Co. (Rockford, IL).

Receptor isolation

Nicotinic acetylcholine receptor-enriched membranes, designated below as nAChR membranes, were isolated from *T. californica* electric organ by established procedures (Johnson and Yguerabide, 1985). The receptor-specific activities were determined by the decrease in dansyltrimethylamine (6.6 μM) fluorescence produced by the titration of suberyldicholine into receptor suspensions (0.3 mg of protein/ml) in the presence of PCP (100 μM), following the method of Neubig and Cohen (1979). The receptor-specific activities ranged between 1.2 and 1.4 nmol/mg of protein.

Synthesis of dansyl-hexanoic acid

5-Dimethylaminonaphthalene-1-sulfonyl chloride (dansyl chloride, 3.7 mmol) in 80 ml of methanol was slowly added to 80 ml of recrystallized 6-aminohexanoic acid (3.7 mmol) in aqueous sodium carbonate (0.8 M). The reaction mixture was incubated for 10 h at ~40°C with continuous stirring and the pH maintained at 9.5 by small additions of sodium carbonate (2.5 M). The reaction mixture was then rotary evaporated, suspended in ~10 ml of ammonium bicarbonate (0.1 M), and applied to a C_{18} reversed-phase flash chromatography (Baker cat. no. 7025-0) column (15 × 3 cm) equilibrated with 0.1 M aqueous ammonium carbonate. The column was sequentially washed with 500 ml each of H_2O, H_2O:CH_3OH (4:1, v/v), H_2O:CH_3OH (2:1, v/v), and H_2O:CH_3OH (1:1, v/v). The fractions associated with the 2:1 H_2O:CH_3OH wash, that contained the desired product, were rotary evaporated to near dryness and lyophilized. The final product was 1.03 g of a yellow powder (3.0 mmol, 73% yield).

Synthesis of dansyl-C_6-choline

Dansyl-hexanoic acid (1.3 mmol) was treated with *N,N*-carbonyldiimidazole (2.7 mmol) in 5 ml of anhydrous *N,N*-dimethylformamide at room temperature until cessation of CO_2 production. *N,N*-Dimethylethanolamine (2.3 mmol), that had been previously treated with ~60 mg of sodium metal, was added to the reaction mixture and incubated for 16 h at 65°C under N_2. The reaction mixture was placed on ice and iodomethane (2 mmol) was added. After 30 min, the reaction mixture was rotary evaporated, dissolved in 5 ml of ethanol, and eluted through an anion exchange (AG-1-X2) column (2 × 2 cm) (1 ml/min) equilibrated in ethanol. The fluorescent fractions were rotary evaporated to yield 1.35 g of a yellow oil (2 mmol, 77% yield). Electrophoresis of the product showed migration of a single fluorescent spot toward the negative pole at both pH 7.0 and 11.0. Silica gel thin layer chromatography ($CHCl_3$:CH_3OH:CH_2COOH:H_2O, 25:12:4:2, v/v) of the product indicated a single fluorescent spot with an R_f = 0.18.

Fluorescence measurements

Steady-state fluorescence measurements were made with an MPF 66 spectrofluorometer (Perkin-Elmer Cetus). Emission correction factors were generated with the aid of a calibrated 150-watt reference lamp from Optronics Laboratories (Orlando, FL). Fluorescence lifetimes were determined by the time-correlated single photon-counting technique using a nanosecond fluorescence spectrofluorometer (EEY scientific; La Jolla, CA), equipped with a high pressure hydrogen arc lamp. A Polaroid HNPB dichroic film polarizer (Norwood, MA), rotated 55° relative to the vertical, was placed in the emission path, and fluorescence decays were analyzed with the GLOBALS UNLIMITED program (version 1.01; Fluorescence Dynamics Laboratory; Urbana-Champaign, IL).

Affinity of specific dansyl-C_6-choline binding to nAChR-enriched membranes

The equilibrium dissociation constant of dansyl-C_6-choline was estimated by the forward titration of dansyl-C_6-choline into nAChR suspensions (50 nM in suberyldicholine binding sites) in buffer I, previously incubated with PCP (40 μM). A parallel sample that was preincubated for 30 min at room temperature with cobra-α-toxin (200 nM) assessed the fluorescence from nonspecifically bound dansyl-C_6-choline. The binding affinities were estimated by fitting plots of the specific fluorescence associated to dansyl-C_6-choline binding to the ACh binding site (cobra-α-toxin-sensitive fluorescence) versus the total ligand concentration to a four-parameter logistic equation (sigmoid) by using the GraphPad computer program (GraphPAD Software; San Diego, CA).

Fractional specific and nonspecific dansyl-C_6-choline association with the nAChR membranes

Dansyl-C_6-choline (0.4 μM) and nAChR membranes (0.4 μM in suberyldicholine binding sites) were suspended in 1.5 ml of buffer I and PCP (100 μM), with and without cobra-α-toxin (4 μM). Parallel samples that contained equivalent concentrations of dansyl-C_6-choline in buffer I or nAChR membranes suspended in buffer I, both in the presence of PCP, were used to determine the total and background fluorescence, respectively. The samples were centrifuged in a Beckman TL-100 ultracentrifuge at 100,000 *g* for 1 h. at room temperature and the supernatant-dansyl-C_6-choline emission was monitored at 550 nm with excitation at 220 nm. In the absence of specific binding the apparent membrane partition coefficient (K_P^*) of dansyl-C_6-choline was calculated with the expression

$$K_P^* = \frac{I_{total} - I^S_{+tox}}{I^S_{+tox}} = \frac{L_P}{L_F} \quad (1)$$

where I is the background-subtracted dansyl fluorescence. The superscript S represents the fluorescence of the supernatants, and the subscripts *total*

and $+tox$ represent the samples that contained only the fluorophore in buffer, fluorophore + nAChR membranes + α-toxin, and nAChR only, respectively. L_P and L_F are the amounts of ligand membrane-partitioned and free, respectively.

The fraction of the dansyl-C_6-choline that specifically binds to the ACh binding sites (f_B) was calculated with the expression

$$f_B = \frac{I_{total} - I^S_{-tox}(1 + K^*_P)}{I_{total}} = \frac{L_B}{L_T} \quad (2)$$

where I^S_{-tox} is the background-subtracted supernatant fluorescence of the samples that contained both fluorophore and nAChR but not α-toxin. L_B and L_T are the amounts of specifically bound and total ligand, respectively.

Quantum yield of nAChR-bound and membrane-partitioned dansyl-C_6-choline

The quantum yield of dansyl-C_6-choline bound to the nAChR (Q_B) was determined by solving Eq. 3 (see Appendix for derivation) for Q_B.

$$Q_B = \frac{(Q_F + K^*_F Q_P)((I_{-tox}/I_{+tox}) + f_B - 1)}{f_B(1 + K^*_P)} \quad (3)$$

where I_{-tox}/I_{+tox} is the ratio of the dansyl-C_6-choline fluorescence intensities in the absence and in the presence of cobra-α-toxin, and Q_P is the quantum yield of membrane partitioned dansyl-C_6-choline. The Q_P of dansyl-C_6-choline was determined with Eq. 4

$$Q_P/Q_F = I_P/I_F \quad (4)$$

where the Q_F is the quantum yield of free dansyl-C_6-choline, and I_P and I_F are the fluorescence intensities of membrane partitioned and free dansyl-C_6-choline, respectively. (Here, it is assumed that the emission and absorption spectra of the partitioned and free dansyl-C_6-choline are the same.) The Q_F was determined by the ratio method of Chen et al. (1965) with fluorescein in 0.1 N NaOH as a standard. I_F was measured directly by using a cuvette that contained dansyl-C_6-choline (0.4 μM) in buffer I. The I_P was determined from a cuvette that contained PCP (100 μM), dansyl-C_6-choline (0.4 μM), cobra-α-toxin (4 μM), and nAChR membranes (0.4 μM in suberyldicholine binding sites) suspended in buffer I. A sample that contained identical concentrations of nAChR membranes, PCP, and cobra-α-toxin was used to subtract the background fluorescence. The background-subtracted fluorescence (I_{obs}) was corrected for inner filter effects (I_{cor}), produced by the light scattering from the membrane fragments, with Eq. 5 (Lakowicz, 1983)

$$I_{cor} = I_{obs} \cdot 2.303 \exp[(OD_{ex} + OD_{em})/2] \quad (5)$$

where OD_{ex} and OD_{em} are the absorbance of the sample at 310 and 540 nm, the excitation and emission wavelengths used to monitor the dansyl-C_6-choline fluorescence.

Fluorescence resonance energy transfer (FRET) model

To calculate the transverse distance between the receptor-bound donors and acceptors randomly positioned at the membrane surface we used the Off-Axis model that assumes that the donors are attached at a distance δ from the major axis of symmetry of cylindrical proteins imbedded into a planar-lipid membrane. The symmetry axis of this protein is perpendicular to the membrane surface. The transverse distance from the protein-bound donors to acceptors positioned in the plane of the water-lipid interface is R_P. The distance of closest approach between the acceptors and the central axis of the protein in the acceptor plane is α, and α is assumed to be greater than or equal to δ. All this is represented graphically in Fig. 1. This model is derived in a more general form elsewhere (see accompanying article by Yguerabide).

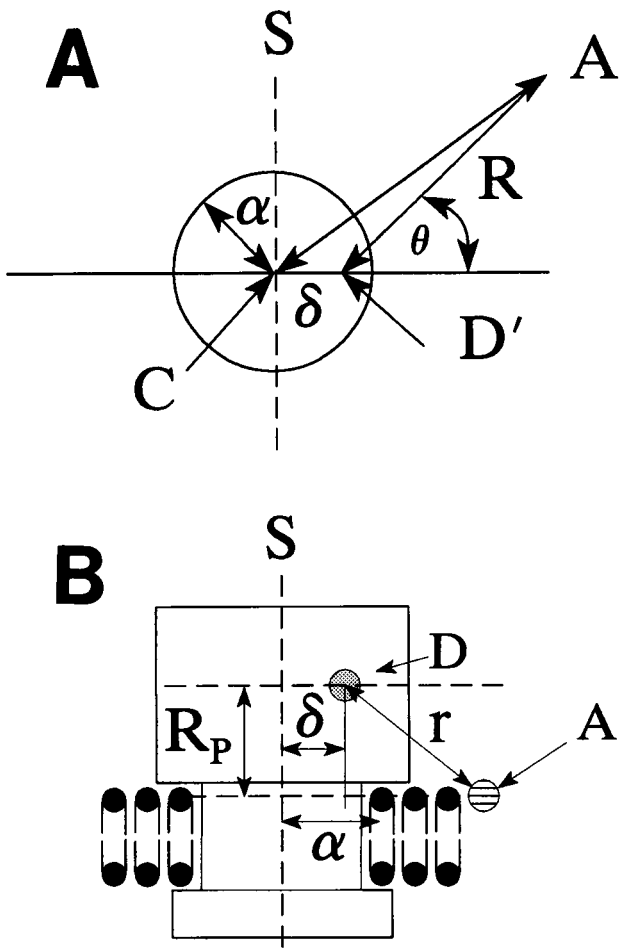

FIGURE 1 Schematic representation of the Off-Axis membrane FRET model. (*A*) Schematic representation in the acceptor plane of the coordinate system used to describe the position of an acceptor A relative to the projection of the donor (*D′*) into the acceptor plane. The radius α of the circle is the distance of closest approach of acceptors to the center of the circle C. The center is the point where the transverse symmetry axis S of the cylindrically symmetric protein intercepts the acceptor plane. δ is the distance from the symmetry axis S at the center of the circle to D′. The position of A with respect to D′ in the acceptor plane is described by the distance R and angle θ. (*B*) Cross-sectional representation of this model. *r* is the distance of closest approach between the donor D and an acceptor A. Membrane-partitioned acceptors are assumed to be distributed randomly in a planar array at a distance R_P below the level of the donors.

To calculate theoretical energy transfer efficiency for this model, the fluorescent lifetime of the donor is represented by τ_D. The donor fluorescence intensity, $F(t)$, at any time t after excitation by a very short pulse of light is given by

$$F(t) = F(0)e^{-t/\tau_D}e^{-\sigma M(t)} \quad (6)$$

where σ is the surface density of acceptors and M(t), in turn, is defined by the following integral

$$M(t) = 2\int_0^\pi S(t, \theta)\, d\theta. \quad (7)$$

$S(t, \theta)$ is given by the integral

$$S(t, \theta) = \int_{r_c(\theta)}^{\infty} (1 - e^{(t/\tau)(R_0/r)^6})r\, dr \quad (8)$$

where r is the distance between donor-acceptor pairs and r_c is the distance of closest approach between donor-acceptor pairs and equals

$$r_c(\theta) = [R_p^2 + R_c^2(\theta)]^{1/2} \quad (9)$$

where

$$R_c(\theta) = -\delta \cos\theta + [\delta^2\cos^2\theta + (\alpha^2 - \delta^2)]^{1/2}. \quad (10)$$

For steady-state emission, the ratio of donor fluorescence in the presence over absence of acceptor (I_D/I_{DA}) is given by the integral ratio

$$\frac{I_D}{I_{DA}} = \frac{\int_0^\infty F_D(t)\,dt}{\int_0^\infty F_{DA}(t)\,dt} \quad (11)$$

where the subscripts *D* and *DA* denote the absence and presence of acceptor, respectively. The surface density of acceptor probes was determined as described in Valenzuela et al., (1992).

FRET measurements

Dansyl-C_6-choline (0.4 μM) and nAChR-associated membranes (0.4 μM in suberyldicholine binding sites) were suspended in buffer I, in the presence of PCP (100 μM). The excess PCP was added to prevent dansyl-C_6-choline from binding to the HNCI site, thereby increasing the specificity of the dansyl-C_6-choline binding. A parallel cuvette that also contained cobra-α-toxin (4 μM) was used to estimate the fluorescence of the nonspecifically bound dansyl-C_6-choline. Titrants were dissolved in dimethyl sulfoxide (which had no measurable effect on dansyl-C_6-choline fluorescence) and were added to the cuvettes with Hamilton syringes. After each addition of titrant, the samples were incubated for 5 min before fluorescence measurements were performed. Initial control experiments demonstrated that the titrants were at equilibrium with the membrane within 5 min. (data not shown). All samples were corrected for intrinsic fluorescence of the acceptors and background fluorescence, as previously described by Valenzuela et al. (1992).

Because only a fraction of the dansyl-C_6-choline (f_B = 0.85) was specifically bound to the ACh binding sites, the determination of the specific FRET to the membrane-partitioned acceptors required separation of the bound donor fluorescence (I_B) from the free and membrane-partitioned donor fluorescence. This was accomplished by using Eq. 12.

$$I_B = I_{-tox} - (1 - f_B)I_{+tox} \quad (12)$$

where I_{-tox} and I_{+tox} are the magnitudes of fluorescence of samples that did not or did contain cobra-α-toxin, respectively (see Appendix for derivation). The observed fluorescence was corrected for dilution and inner filter effects of the acceptor. The fraction of dansyl-C_6-choline that was not bound to the ACh binding sites ($1 - f_B$) was determined with the centrifugation assay described above.

For the FRET experiments, the dansyl-C_6-choline was excited at 310 nm instead of 340 nm for direct excitation or 280 nm for indirect-dansyl excitation through the receptor tryptophans. This was done both to enhance receptor-bound dansyl-C_6-choline fluorescence (310-nm excitation yields about 50% greater receptor-bound dansyl fluorescence than 340 nm), and to avoid indirect excitation of dansyl via a FRET process between receptor tryptophans and receptor-bound dansyl-C_6-choline. FRET between receptor tryptophans and dansyl-C_6-choline was avoided, because the lipophilic acceptors used directly quench nAChR tryptophans fluorescence (unpublished observation) and, thereby, indirectly quench receptor-bound dansyl-C_6-choline fluorescence. Indirect tryptophan-to-dansyl excitation inappropriately enhances the dansyl-C_6-choline quenching. Evidence that 310-nm excitation does not produce significant indirect tryptophan-to-dansyl excitation comes from the fact that the dansyl-C_6-choline fluorescence in the absence of cobra-α-toxin divided by its fluorescence in the presence of the toxin (I_{-tox}/I_{+tox}) is essentially the same whether or not the samples are excited at 310 nm (I_{-tox}/I_{+tox} = 2.1 ± 0.4; 13 determinations) or 340 nm (I_{-tox}/I_{+tox} = 2.3 ± 0.6; seven determinations). Excitation at 280 nm is associated with 6.9 ± 0.5 fold (four determinations) increase in dansyl-C_6-choline fluorescence (data not shown).

RESULTS

K_d for dansyl-C_6-choline binding to the ACh sites

The concentration-dependent change in dansyl-C_6-choline fluorescence that is associated with its binding to the ACh binding sites (cobra-α-toxin-sensitive fluorescence) is shown in Fig. 2. A nonlinear fit of this data to a four-parameter logistic equation (sigmoid) yielded a K_d of 20 ± 14 nM. This value is in reasonable agreement with the K_d = 10 nM measured by the decrease in the initial velocity of [^{3}H]α-toxin binding to receptor-enriched microsacs (Heidmann and Changeux, 1979a).

Fractional specific and nonspecific association of dansyl-C_6-choline with nAChR membranes

Following centrifugation of samples containing dansyl-C_6-choline and nAChR membranes, the background-subtracted, supernatant-dansyl fluorescence was reduced by 88 ± 2% when compared to samples that did not contain nAChR membranes (Table 1). When cobra-α-toxin was preincubated in parallel samples, supernatant-dansyl fluorescence was only reduced 19 ± 3% (Table 1). Because the total volumes of membranes and solvent remained constant, the ratio of membrane-partitioned/free dansyl-C_6-choline should remain constant with and without cobra-α-toxin. Consequently, under the conditions in which the FRET experiments (described below) were performed, the fraction of dansyl-C_6-choline that was specifically bound to the ACh binding sites was (f_B =) 0.85 (Eq. 2), and the apparent partition coefficient (K_P^*) of dansyl-C_6-choline was calculated (Eq. 1) to be 0.24. This means that when dansyl-C_6-choline is allowed to bind

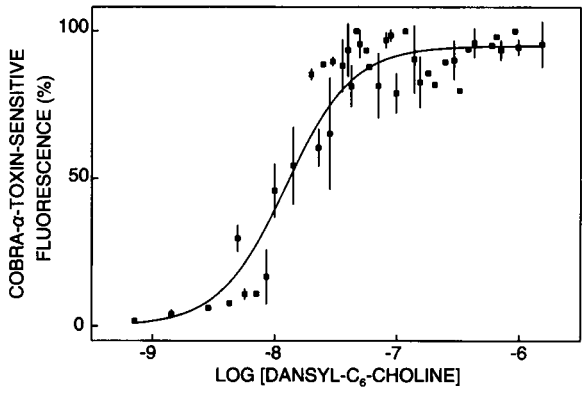

FIGURE 2 Concentration dependence of specific dansyl-C_6-choline binding to the nAChR. Incremental amounts of dansyl-C_6-choline were titrated into suspensions of nAChR (50 nM in suberyldicholine binding sites) previously incubated for 10 min with PCP (40 μM), in the absence and in the presence of an excess of cobra-α-toxin (200 nM). The numerical difference between the samples without and with α-toxin (average of nine determinations ± standard deviation) is plotted and represents the cobra-α-toxin sensitive fluorescence, which is associated with dansyl-C_6-choline binding to the ACh binding sites. The excitation and emission wavelength were 280 and 540 nm, respectively. The K_d value was 20 ± 14 nM and the Hill slope was 1.7 ± 0.6. The solid line was drawn using the best fit parameters to a four-parameter logistic equation (sigmoid).

TABLE 1 Specific and nonspecific association of dansyl-C_6-choline to the nAChR membranes

	Dansyl-C_6-choline + PCP (I_{total})	Dansyl-C_6-choline + PCP + nAChR (I_{-tox})	Dansyl-C_6-choline + PCP + nAChR + α-toxin (I_{+tox})
Supernatant fluorescence	245.1 ± 4.1	28.1 ± 6.6	198.0 ± 13.5

Shown is the background-subtracted dansyl fluorescence of the supernatants of samples that contained dansyl-C_6-choline (0.4 μM) and PCP (100 μM) ± nAChR membranes (0.4 μM in suberyldicholine binding sites) and ± cobra-α-toxin (4 μM) suspended in buffer I and that were centrifuged at 100,000 *g* for 1 h. The dansyl fluorescence of the supernatants was monitored at 550 nm with excitation at 220 nm. The results are the average ± SD of four determinations.

to the receptor in the energy transfer experiments described below, about 90% of the observed fluorescence is from receptor-bound dansyl-C_6-choline.

Energy transfer parameters

The quantum yield of nAChR-bound dansyl-C_6-choline (Q_B) using Eq. 3 was calculated to be 0.22. This is essentially the same value (0.21) obtained independently by multiplying the ratio of fluorescence lifetimes of dansyl-C_6-choline in the presence to absence of nAChR membranes (8.6/3.0 ns) by the quantum yield of dansyl-C_6-choline in buffer I (0.073) (data not shown). The spectral overlap between nAChR-bound dansyl-C_6-choline and the membrane acceptors, C_{12}-eosin and C_{18}-rhodamine, is shown in Fig. 3. The absorption spectra of the nAChR-partitioned membrane acceptors could not be measured because of the turbidity of the samples. Instead, the fluorescence excitation spectrum of the membrane-associated fluorophores was used to represent the spectral profile of the respective absorption spectrum. The maximum extinction coefficients for C_{12}-eosin and C_{18}-rhodamine were assumed equal to 85,000 and 94,000 cm^{-1} M^{-1}, respectively (Haugland, 1992). The values of the overlap integral for the dansyl-C_6-choline/C_{18}-rhodamine and the dansyl-C_6-choline/C_{12}-eosin donor/acceptor pairs, were 3.7×10^{-13} and 2.5×10^{-13} cm^6/mol, respectively (Table 2). The calculated Förster critical distances for the two donor-acceptor pairs were 48 and 45 Å, respectively.

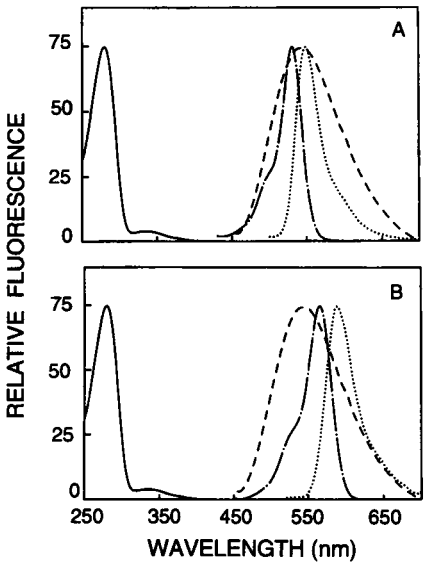

FIGURE 3 Spectral overlap of nAChR-bound dansyl-C_6-choline and C_{12}-eosin or C_{18}-rhodamine (membrane-partitioned acceptors). Shown are the excitation spectra of the donor (——), excitation spectra of the acceptor (— · —), emission spectra of the donor (– – – –), and emission spectra of the acceptor (·····). The donor is dansyl-C_6-choline (100 nM). The acceptors (400 nM) are C_{12}-eosin (panel A) and C_{18}-rhodamine (*B*). All measurements were made with nAChR-associated membranes (200 nM in suberyldicholine binding sites) that had been preincubated with PCP (100 μM). A sample that contained an excess of cobra-α-toxin (6 μM) and dansyl-C_6-choline (100 nM) was used to obtain the spectra of nonspecifically bound dansyl-C_6-choline. These spectra were subtracted to obtain the spectra of specifically bound dansyl-C_6-choline. A cuvette that only contained nAChR membranes was used to assess the background fluorescence for the C_{18}-rhodamine and C_{12}-eosin samples.

Energy transfer between dansyl-C_6-choline and the lipid membrane probes

The concentration dependence of the uncorrected donor quenching of nAChR-bound dansyl-C_6-choline is shown in Fig. 4. (Assuming that the lipid/probe ratio (w/w) of the samples used for these experiments was 0.41 (Gonzalez-Ros et al., 1982) and that the average molecular weight of the nAChR membrane lipids is 800, then at the highest concentration of probe used (6.8 μM) the molar lipid/probe ratio would be about 25:1.) The highest concentrations of C_{18}-rhodamine and C_{12}-eosin produced about a 15 and 25% decrease in the uncorrected nAChR-bound dansyl-C_6-choline fluorescence, respectively. In the presence of cobra-α-toxin, the highest concentrations of C_{18}-rhodamine and C_{12}-eosin produced only about an 8 and 16% decrease in the fluorescence of nonspecifically bound dansyl-C_6-choline, respec-

TABLE 2 Energy transfer parameters for the donor dansyl-C_6-choline and the membrane-partitioned acceptors C_{18}-rhodamine and C_{12}-eosin

Acceptor	J^* ($\times 10^{13}$)	R_O‡	R_P§
	cm^6/mol	Å	Å
C_{18}-rhodamine	3.7	48	39 ± 6
C_{12}-eosin	2.5	45	31 ± 5

* Overlap integral equals $\Sigma I_B(\lambda)\epsilon_A(\lambda)\lambda^{-4}\Delta\lambda/\Sigma I_B(\lambda)\Delta\lambda$ where $\epsilon_A(\lambda)$ is the extinction coefficient of the acceptor. The quantum yield of receptor-bound dansyl-C_6-choline was determined as described under Experimental Procedures (Q_B = 0.22).

‡ Förster critical distance equals $9.765 \times 10^3(Q_B n^{-4}\kappa^2 J)^{1/6}$ (assumptions: $\kappa^2 = \frac{2}{3}$ and n = 1.4).

§ Mean ± SD transverse distance to lipophilic fluorophores in membrane calculated as described in Experimental Procedures (Eqs. 6–11).

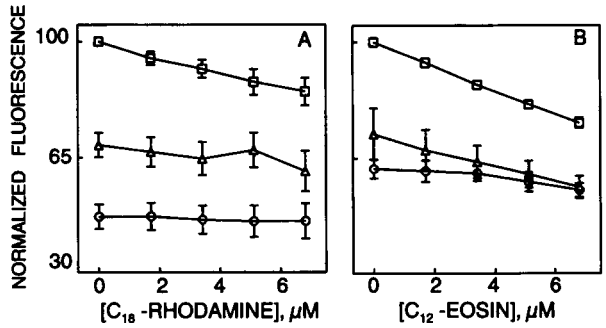

FIGURE 4 Effect of C_{18}-rhodamine or C_{12}-eosin on dansyl-C_6-choline fluorescence in the absence and in the presence of cobra-α-toxin. Plotted is the fluorescence of nAChR-bound dansyl-C_6-choline (□) as a function of various concentrations of membrane-partitioned acceptors, C_{18}-rhodamine (*A*) or C_{12}-eosin (*B*). The effect of the added C_{18}-rhodamine or C_{12}-eosin on the fluorescence of samples that additionally contained nAChR-bound cobra-α-toxin (; 4 μM) or that only contained nAChR (○) is also shown. The concentrations of nAChR in suberyldicholine binding sites, dansyl-C_6-choline, and PCP were 0.4, 0.4, and 100 μM, respectively. The excitation wavelength was 310 nm (3-nm slit) in all cases. The emission wavelengths were 500 and 540 nm for the experiments with C_{12}-eosin and C_{18}-rhodamine, respectively. The emission slit was 5 nm in all cases. These emission wavelengths were chosen to minimize the detection of acceptor fluorescence. Corrections were made for dilution. Each datum point represents the average ± standard deviation of three determinations.

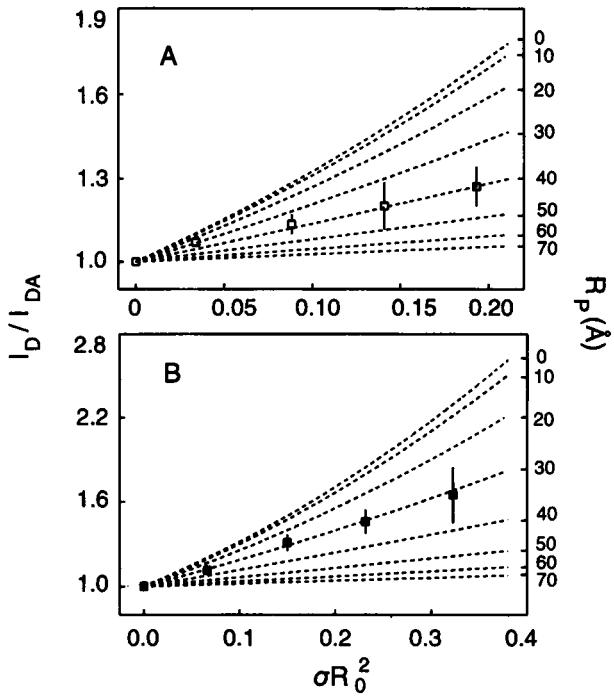

FIGURE 5 Energy transfer between dansyl-C_6-choline and the membrane-partitioned C_{18}-rhodamine and C_{12}-eosin. Plotted as points ± standard deviations (three determinations) are the average ratios of nAChR-bound dansyl-C_6-choline (donor) fluorescence, in the absence (I_D) and in the presence (I_{DA}) of the membrane-partitioned acceptors, C_{18}-rhodamine (□, *A*) or C_{12}-eosin (■, *B*), as a function of the surface density of acceptors (σ) times the σR_0^2. Plotted as a series of dotted lines are the numerically calculated relation between I_D/I_{DA} and σR_0^2 for discrete donors above a planar distribution of acceptors with a transverse distance (R_P) ranging between 0–70 Å (Eqs. 6–11; $\alpha = \delta = 27$ Å). The fluorescence of dansyl-C_6-choline bound to the nAChR was calculated with Eq. 8. The surface density of acceptors (σR_0^2) was determined as described under Experimental Procedures. For more details see legend for Fig. 3.

tively. The change in the fluorescence of the sample produced by the intrinsic fluorescence of the membrane-acceptors was very small or insignificant.

The calculated (Eq. 12) nAChR-bound dansyl-C_6-choline fluorescence in the absence (Q_D) of acceptors was divided by its fluorescence in the presence (Q_{DA}) of the acceptors, C_{12}-eosin or C_{18}-rhodamine, and was plotted as a function of the surface density of acceptors, σ, times R_0^2 (Fig. 5). For comparison, theoretical plots of Q_D/Q_{DA} vs. σR_0^2 were calculated numerically and are also shown for various values of the transverse distance (R_P, with Eqs. 6–11). Analysis of the slopes of the experimental data in relation to the theoretical lines yielded R_P values of 39 and 31 Å for the dansyl-C_6-choline/C_{18}-rhodamine and the dansyl-C_6-choline/C_{12}-eosin pairs, respectively (Table 2).

As a control to establish the stability of the receptor-bound dansyl-C_6-choline fluorescence, a suspension of the *Torpedo* membranes and dansyl-C_6-choline was prepared and monitored for 2 h, the time to perform the FRET experiments described above. No significant decrement of the dansyl-C_6-choline fluorescence was observed (data not shown).

DISCUSSION

In the present study, FRET techniques were used to estimate the transverse distance between the two ACh binding sites on the *Torpedo* nAChR and the surface of the lipid membrane. The energy donor was dansyl-C_6-choline, a well characterized fluorescent agonist that binds with high affinity (K_d ~10^{-8} M) to the ACh binding sites on the nAChR (Heidmann and Changeux, 1979a, b). Dansyl-C_6-choline, like other nicotinic agonists, depolarizes isolated electroplax from *Electrophorus electricus* and increases $^{22}Na^+$ efflux from receptor-enriched microsacs obtained from *Torpedo marmorata* (Heidmann and Changeux, 1979a).

With dansyl-C_6-choline as a donor, the average calculated transverse distance between the ACh binding sites and the chromophoric portions of C_{12}-eosin or C_{18}-rhodamine partitioned into the membrane was ~35 Å (illustrated in Fig. 6).

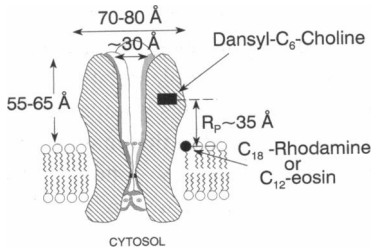

FIGURE 6 Schematic representation of the location of the ACh binding sites on the nAChR (following Unwin (1993)). R_P, the transverse distance between the receptor-bound donor and the membrane-partitioned acceptors positioned at the water-lipid interface, was found to be 30–39 Å.

This value is substantially less than the maximum extracellular protrusion of the nAChR (55–65 Å), and therefore supports the idea that the ACh binding sites are localized substantially below the apex of the extracellular protrusion of the receptor. The recent 9-Å resolution structural analysis of the nAChR (Unwin, 1993) shows a pocket in about the center of each α-subunit, ~30 Å above the surface of the membrane. These pockets were postulated to correspond to the ACh binding sites, which is consistent with the present finding that the ACh binding sites are located ~35 Å above the membrane surface. Clearly, more research is necessary to confirm that the ACh binding sites are located in these pockets, because biochemical data indicate that the ACh sites are at the α-γ and α-δ subunit interfaces (Chatrenet et al., 1990; Pedersen and Cohen, 1990; Middleton and Cohen, 1991; Czajkowski and Karlin, 1991; Czajkowski et al., 1993)

If the ACh binding sites are in these pockets, then structurally complex arrangements of the extracellular domains of one or more subunits would probably be required for the formation of each ACh binding site. Consistent with structurally complex ACh binding sites are affinity labeling (Kao et al., 1984; Dennis et al., 1988; Abramson et al., 1989; Galzi et al., 1990; Pedersen and Cohen, 1990; Cohen et al., 1991; Middelton and Cohen, 1991) and site-directed mutagenesis studies (Tomaselli et al., 1991) that demonstrate contributions from more than one segment of the NH_2-terminal extracellular domains of the α, δ, and γ subunits to the formation of the ACh binding sites.

There are several issues that must be considered in the interpretation of these findings. First, the model that was used to analyze the FRET data assumes that there is a random distribution of the membrane acceptors. If the lipophilic acceptors can differentially associate with the receptor, it would lead to a nonrandom distribution of acceptors in the membranes. Steroids and negatively charged fatty acids display 3–5-fold greater affinity for the receptor than the zwitterionic phosphatidylcholine (Ellena et al., 1983). It is reasonable to expect that negatively charged C_{12}-eosin and positively charged C_{18}-rhodamine differentially associate with the receptor. However, despite possible differences in the association of C_{12}-eosin and C_{18}-rhodamine to the receptor, the calculated distances of closest approach using two differently charged acceptors were within ~9 Å of each other, which illustrates that the method used is only weakly dependent on the random distribution of the acceptors in the membrane. Second, FRET studies usually are associated with the problem of not knowing the orientation (κ^2) of the donor-emission transition dipole relative to the acceptor-absorption transition dipole. This is not a significant problem in the experiments described in this manuscript, because the energy transfer between energy donors and acceptors involves both static and dynamic averaging (Dale et al., 1979; Johnson et al., 1990). Moreover, although we used two acceptors which would presumably have different transition dipole orientations, we still observed the same magnitude of energy transfer to each acceptor after correcting for R_o and surface density.

In summary, our measurements suggest that the ACh binding sites are located significantly below the extracellular apex of the receptor, probably at a site equidistant from the extracellular end and the beginning of the transmembrane domain (Fig. 6). The FRET determinations presented above, support the recently proposed location for the ACh binding sites in two pockets, ~30 Å above the membrane surface (Unwin, 1993), and should contribute to our understanding of ligand-regulated gating of the nAChR and of other members of this ion channel superfamily.

APPENDIX

When dansyl-C_6-choline, L, can specifically bind to membrane-associated receptors ($L_B > 0$),

$$L_T = L_F + L_P + L_B. \tag{A1}$$

Introducing $L_B = L_T \cdot f_B$ (see Eq. 2) into Eq. A1 and solving for $L_F + L_P$ we get

$$L_F + L_P = (1 - f_B)L_T. \tag{A2}$$

Introducing the expression

$$K_P^* = L_P/L_F \tag{A3}$$

into Eq. A2 and solving for L_F and L_P gives

$$L_P = \frac{K_P^*}{1 + K_P^*}(1 - f_B)L_T \tag{A4}$$

and

$$L_F = \frac{1}{1 + K_P^*}(1 - f_B)L_T. \tag{A5}$$

When L is prevented from specifically binding to the receptor by the presence of excess inhibitor (in the present case cobra-α-toxin), L_B equals zero and the total amount of ligand is equal to

$$L_T = L_F + L_P. \tag{A6}$$

Rearranging and substituting Eq. A3 into Eq. A6 and solving for L_F and L_P gives

$$L_F = \frac{1}{1 + K_P^*}L_T \tag{A7}$$

and

$$L_P = \frac{K_P^*}{1 + K_P^*}L_T. \tag{A8}$$

The steady-state fluorescence of L_F equals

$$I_F = Q_F k\epsilon \frac{L_F}{V} \tag{A9}$$

where V is the sample volume, k is an instrument constant, ϵ is the absorbance, and Q_F is the quantum yield of L_F. The fluorescence of free $L(I_F)$ in the absence of an excess of inhibitor (in this case cobra-α-toxin) can be derived by substituting Eq. A5 into Eq. A9 and equals

$$I_F = \frac{1}{1 + K_P^*}(1 - f_B)Q_F k\epsilon \frac{L_T}{V}. \tag{A10}$$

(Here and below ϵ is assumed to be the same when L is free, bound, or membrane-partitioned.)

Similarly, in the presence of the inhibitor that prevents the specific binding of L, the fluorescence of free ligand (I_F') can be expressed by substituting Eq. A7 into Eq. A9 and equals

$$I_F' = \frac{1}{1 + K_P^*}Q_F k\epsilon \frac{L_T}{V}. \tag{A11}$$

Similarly, the fluorescence of membrane partitioned ligand (I_P) in the absence of inhibitor is given by substituting Eq. A4 into Eq. A9 in which I_F and L_F are replaced with I_P and L_T to yield

$$I_P = \frac{K_P^*}{1 + K_P^*}(1 - f_B)Q_P k\epsilon \frac{L_T}{V}. \quad \text{(A12)}$$

In the presence of inhibitor, the fluorescence of membrane partitioned ligand (I_P') can be derived by substituting Eq. A8 into Eq. A9 in which I_F and L_F are replaced with I_P' and L_T to give

$$I_P' = \frac{K_P^*}{1 + K_P^*} Q_P k\epsilon \frac{L_T}{V}. \quad \text{(A13)}$$

Similarly, I_B equals

$$I_B = f_B Q_B k\epsilon \frac{L_T}{V}. \quad \text{(A14)}$$

For samples that do not contain inhibitor, the total steady-state fluorescence of L in the absence of an excess of a nonfluorescent inhibitor (I_{-tox}) is simply the sum of the fluorescence from bound, membrane-partitioned, and free L. I_{-tox} can, therefore, be represented as

$$I_{-tox} = f_B Q_B k\epsilon \frac{L_T}{V} + \frac{K_P^*(1 - f_B)}{(1 + K_P^*)} Q_P k\epsilon \frac{L_T}{V} + \frac{(1 - f_B)}{(1 + K_P^*)} Q_F k\epsilon \frac{L_T}{V}. \quad \text{(A15)}$$

Similarly, in the presence of the inhibitor where there is no bound L, the fluorescence of L(I_{+tox}) is only the sum of the fluorescence from membrane-partitioned and free L and can be represented as

$$I_{+tox} = \frac{K_P^*}{1 + K_P^*} Q_P k\epsilon \frac{L_T}{V} + \frac{1}{1 + K_P^*} Q_F k\epsilon \frac{L_T}{V}. \quad \text{(A16)}$$

The rearrangement of Eq. A15 gives

$$I_B = I_{-tox} - \left(\frac{1 - f_B}{1 + K_P^*} k\epsilon \frac{L_T}{V}\right)(K_P^* Q_P + Q_F). \quad \text{(A17)}$$

The rearrangement of Eq. A16 gives

$$\frac{I_{+tox}(1 + K_P^*)}{k\epsilon L_T/V} = K_P^* Q_P + Q_F \quad \text{(A18)}$$

and the substitution of Eq. A18 into A17 gives

$$I_B = I_{-tox} - I_{+tox}(1 - f_B). \quad \text{(A19)}$$

This shows that I_B can be calculated without knowledge of the nonspecific membrane-partitioning of the ligand or quantum yields of the ligand in different microenvironments.

The quantum yield of the specifically bound ligand (Q_B) can be determined by taking the ratio of I_{-tox} (Eq. A15) over I_{+tox} (Eq. A16) and rearranging to solve for Q_B giving

$$Q_B = \frac{(Q_F + K_P^* Q_P[(I_{-tox}/I_{+tox}) - 1 + f_B]}{f_B(1 + K_P^*)}. \quad \text{(A20)}$$

We are grateful to Dũng Nguyen for assistance with the preparation of the nAChR membranes.

REFERENCES

Abramson, S. N., Y. Li, P. Culver, and P. Taylor. 1989. An analog of lophotoxin reacts covalently with Tyr^{190} in the α-subunit of the nicotinic acetylcholine receptor. *J. Biol. Chem.* 264:12666–12672.

Arias, H. R., C. F. Valenzuela, and D. A. Johnson. 1993. Transverse localization of the quinacrine binding site on the *Torpedo* acetylcholine receptor. *J. Biol. Chem.* 268:6348–6355.

Chatrenet, B., O. Tremeau, F. Bontems, M. P. Goeldner, C. G. Hirth, and A. Menez. 1990. Topography of toxin-acetylcholine receptor complexes by using photoactivable toxin derivatives. *Proc. Natl. Acad. Sci. USA.* 87:3378–3382.

Chen, R. F. 1965. Fluorescence quantum yield measurements: vitamin B_6 compounds. *Science (Wash. DC).* 150:1593–1595.

Cohen, J. B., S. D. Sharp, and W. S. Liu. 1991. Structure of the agonist binding site of the nicotinic acetylcholine receptor. *J. Biol. Chem.* 266: 23354–23364.

Czajkowski, C., and A. Karlin. 1991. Agonist binding site of *Torpedo* electric tissue nicotinic acetylcholine receptor: a negatively charged region of the δ subunit within 0:9 nm of the α subunit binding site disulfide. *J. Biol. Chem.* 266:22603–22612.

Czajkowski, C., C. Kaufmann, and A. Karlin. 1993. Negatively charged amino acid residues in the nicotinic receptor δ subunit that contribute to the binding of acetylcholine. *Proc. Natl. Acad. Sci. USA.* 90:6285–6289.

Dale, R. E., J. Eisinger, and W. E. Blumberg. 1979. The orientation factor in intramolecular energy transfer *Biophys. J.* 26:161–194.

Dennis, M., J. Giraudat, F. Kotzyba-Hybert, M. Goeldner, C. Hirth, J. Y. Chang, C. Lazure, M. Chretien, and J.-P. Changeux. 1988. Amino acids of the *Torpedo marmorata* acetylcholine receptor labeled by a photoaffinity ligand for the acetylcholine binding site. *Biochemistry.* 27: 2346–2357.

Ellena, J. F., M. A. Blazing, and M. McNamee. 1983. Lipid-protein interactions in reconstituted membranes containing acetylcholine receptor. *Biochemistry.* 22:5523–5535.

Förster, T. 1959. Transfer mechanisms of electronic excitation. *Discuss. Faraday Soc.* 27:7–17.

Galzi, J.-L., F. Revah, A. Bessis, and J.-P. Changeux. 1991. Functional architecture of the nicotinic acetylcholine receptor: from electric organ to brain. *Annu. Rev. Pharmacol.* 31:37–72.

Galzi, J.-L., F. Revah, D. Black, M. Goeldner, C. Hirth, and J.-P. Changeux. 1990. Identification of a novel amino acid α-tyrosine 93 within the cholinergic ligands-binding sites of the acetylcholine receptor by photoaffinity labeling. *J. Biol. Chem.* 265:10430–10437.

Gonzalez-Ros, J. M., M. Llanillo, A. Paraschos, and M. Martinez-Carrion. 1982. Lipid environment of the acetylcholine receptor from *Torpedo californica*. *Biochemistry.* 21:3467–3474.

Haugland, R. P. 1992. *Handbook of Fluorescent Probes and Research Chemicals*, 5th Ed. Molecular Probes Inc, Eugene OR. 421 pp.

Heidmann, T., and J.-P. Changeux. 1979a. Fast kinetics studies on the interaction of a fluorescence agonist with the membrane-bound acetylcholine receptor. *Eur. J. Biochem.* 94:255–279.

Heidmann, T., and J.-P. Changeux. 1979b. Fast kinetic studies on the allosteric interactions between acetylcholine receptor and local anesthetic binding sites. *Eur. J. Biochem.* 94:281–296.

Herz, J. M., and S. J. Atherton. 1992. Steric factors limit access to the noncompetitive inhibitor site of the nicotinic acetylcholine receptor. *Biophys. J.* 62:74–76.

Herz, J. M., D. A. Johnson, and P. Taylor. 1987. Interaction of noncompetitive inhibitors with the acetylcholine receptor. *J. Biol. Chem.* 262: 7238–7247.

Herz, J. M., D. A. Johnson, and P. Taylor. 1989. Distance between the agonist and noncompetitive inhibitor sites on the nicotinic acetylcholine receptor. *J. Biol. Chem.* 264:12439–12448.

Herz, J. M., S. J. Kolb, T. Erlinger, and E. Schmid. 1991. Channel permeant cations selectively compete with noncompetitive inhibitors of the nicotinic acetylcholine receptor. *J. Biol. Chem.* 266:16691–16698.

Kao, P., A. Dwork, R. Kaldany, M. Silver, J. Wideman, S. Stein, and A. Karlin. 1984. Identification of the α-subunit half-cystine specifically labeled by an affinity reagent for the acetylcholine receptor binding site. *J. Biol. Chem.* 259:11662–11665.

Karlin, A. 1991. Explorations of the nicotinic acetylcholine receptor. *Harvey Lect.* 85:71–107.

Johnson, D. A., and J. Yguerabide. 1985. Solute accessibility to N^{ϵ}-fluorescein isothiocyanate-$lysine^{23}$ cobra-α-toxin bound to the acetylcholine receptor. *Biophys. J.* 48:949–955.

Johnson, D. A., R. Cushman, and R. Malekzadeh. 1990. Orientation of cobra-α-toxin on the nicotinic acetylcholine receptor. *J. Biol. Chem.* 265: 7360–7368.

Karlsson, E., H. Arnberg, and P. Eaber, 1971. Isolation of the principal neurotoxins of two *Naja* subspecies. *Eur. J. Biochem.* 21:1–16.

Kistler, J., R. M. Stroud, M. W. Klymkowsky, R. A. Lalancette, and R. H.

Fairclough. 1982. Structure and function of an acetylcholine receptor. *Biophys. J.* 37:371–383.

Klymkowsky, M. W., and R. M. Stroud. 1979. Immunospecific identification and three-dimensional structure of a membrane-bound acetylcholine receptor from *Torpedo californica*. *J. Mol. Biol.* 128: 319–334.

Kubalek, E., S. Ralston, J. Lindstrom, and N. Unwin. 1987. Location of subunits within the acetylcholine receptor by electron image analysis of tubular crystal from *Torpedo marmorata*. *J. Cell. Biol.* 105:9–18.

Middleton, R. E., and J. B. Cohen. 1991. Mapping of the acetylcholine binding site of the nicotinic acetylcholine receptor: [^{3}H]nicotine as an agonist photoaffinity label. *Biochemistry*. 30:6987–6997.

Mitra, A. K., M. P. McCarthy, and R. E. Stroud. 1989. Three dimensional structure of the nicotinic acetylcholine receptor and location of the major associated 43-kD cytoskeletal protein, determined at 22 Å by low dose electron microscopy and X-ray diffraction to 12:5 Å. *J. Cell. Biol.* 109: 755–774.

Neubig, R. R., and J. B. Cohen. 1979. Equilibrium binding of [^{3}H]tubocurarine and [^{3}H]acetylcholine by *Torpedo* postsynaptic membranes: stoichiometry and ligand interactions. *Biochemistry*. 18:5464–5475.

Pedersen, S. E., and J. B. Cohen. 1990. D-Tubocurarine binding sites are located at α-γ and α-δ subunit interfaces of the nicotinic acetylcholine receptor. *Proc. Natl. Acad. Sci. USA*. 87:2785–2789.

Sterz, R., M. Hermes, K. Peper, and R. J. Bradley. 1982. Effects of ethidium bromide on the nicotinic acetylcholine receptor. *Eur. J. Pharmacol.* 80: 393–399.

Stroud, R. M., M. P. McCarthy, and M. Shuster. 1990. Nicotinic acetylcholine receptor superfamily of ligand-gated ion channels. *Biochemistry*. 29:11009–11023.

Taylor, P., S. Abramson, D. A. Johnson, C. F. Valenzuela, and J. Herz. 1991. Distinctions in ligand binding sites on the nicotinic acetylcholine receptor. *Ann. N.Y. Acad. Sci.* 625:568–587.

Tomaselli, G. F., J. T. McLaughlin, M. E. Jurman, E. Hawrot, and G. Yellen. 1991. Mutations affecting agonist sensitivity of the nicotinic acetylcholine receptor. *Biophys. J.* 60:721–727.

Unwin, N. 1993. The nicotinic acetylcholine receptor at 9 Å resolution. *J. Mol. Biol.* 229:1101–1124.

Valenzuela, C. F., J. A. Kerr, and D. A. Johnson. 1992. Quinacrine binds to the lipid-protein interface of the *Torpedo* acetylcholine receptor: a fluorescence study. *J. Biol. Chem.* 267:8338–8244.

Walkinshaw, M. D., W. Saenger, and A. Maelicke. 1980. Three-dimensional structure of the "long" neurotoxin from cobra venom. *Proc. Natl. Acad. Sci. USA*. 77:2400–2404.

Yguerabide, J. 1994. Theory for establishing proximity relations in membrane excitation energy transfer measurements. *Biophys. J.* 66: 683–693.

Zingsheim, H. P., F. J. Barrantes, J. Frank, W. Hänicke, and D.-Ch. Neugebauer. 1982. Direct structural localization of two toxin-recognition sites on an ACh receptor protein. *Nature (Lond.)*. 299:81–84